Science of the Total Environment 784 (2021) 147057

Contents lists available at ScienceDirect

Science of the Total Environment

journal homepage: www.elsevier.com/locate/scitotenv

Predicting Paradise: Modeling future wildfire disasters in the western US

Alan A. Ager [a,*], Michelle A. Day [a], Fermin J. Alcasena [b], Cody R. Evers [c], Karen C. Short [a], Isaac Grenfell [a]

[a] *USDA Forest Service, Rocky Mountain Research Station, Missoula Fire Sciences Laboratory, Missoula, MT, USA*
[b] *USDA Forest Service International Visitor Program, Oregon State University, College of Forestry, Forest Ecosystems & Society, Corvallis, OR, USA*
[c] *Portland State University, Environmental Science and Management, Portland, OR, USA*

HIGHLIGHTS

- We used wildfire simulation data to predict building exposure in the western US.
- We examined the relative effect of building versus fuel density on exposure.
- Maximum exposure was observed at building densities between 1400 and 1500 per km^2.
- Building-fuels density gradients into developed areas affected maximum exposure.
- Annual building exposure in extreme fire seasons exceeded historical by 1255%.

GRAPHICAL ABSTRACT

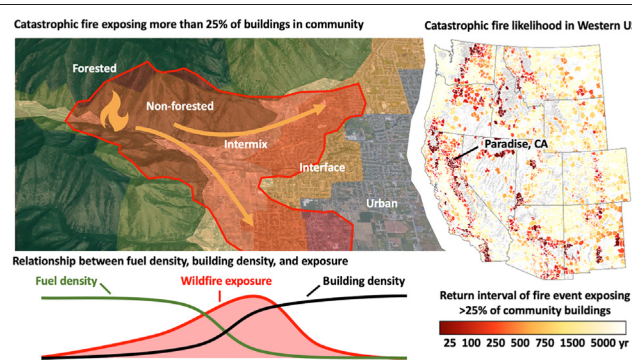

ARTICLE INFO

Article history:
Received 15 December 2020
Received in revised form 5 April 2021
Accepted 7 April 2021
Available online 13 April 2021

Editor: Paulo Pereira

Keywords:
Wildfire transmission
Wildland urban interface
Community exposure
Extreme event
Risk assessment

ABSTRACT

The 2018 Camp fire destroyed the town of Paradise, California and resulted in 82 fatalities, the worst wildfire disaster in the US to date. Future disasters of similar or greater magnitude are inevitable given predicted climate change but remain highly uncertain in terms of location and timing. As with other natural disasters, simulation models are one of the primary tools to map risk and design prevention strategies. However, risk assessments have focused on estimation of mean values rather than predicting extreme events that are increasingly becoming a reality in many parts of the globe. Using the western US as a study area, we synthesized newer wildfire simulation and building location data (54 million fires, 25 million building locations) and compared the outputs to several sources of observed exposure data. The simulations used synchronized weather among spatial simulation subunits, thereby providing estimates of extreme fire seasons, fire events within them, and exceedance probabilities at multiple scales. We found that annual area burned was accurately replicated by simulations but building exposure was substantially overestimated, although the relatively small historical sample size might have influenced the comparison. We identified extreme fire seasons in the simulation record (10,000 fire years) that exceeded historical fire seasons by 278% in terms of area burned, and 1255% in terms of buildings exposed, under contemporary climate. Simulated building exposure peaked in specific regions along gradients of building density and burnable fuels. The study is the first to explore large scale extreme wildfire exposure in terms of both annual variability and magnitude, providing a broad foundation of methods to advance wildfire disaster prediction.

Published by Elsevier B.V.

1. Introduction

Predictive mapping of extreme wildfire disasters presents a daunting challenge to the field of risk and hazard science (Makridakis and Taleb, 2009; Tedim et al., 2018). Wildfire risk to developed areas is the

* Corresponding author.
E-mail address: alan.ager@usda.gov (A.A. Ager).

https://doi.org/10.1016/j.scitotenv.2021.147057
0048-9697/Published by Elsevier B.V.

cumulative product of complex interacting factors including spatiotemporal patterns of human and natural ignitions, fire propagation over long distances through heterogeneous fuel types and terrain, extreme weather events, variation in building susceptibility, and suppression capacity (Alcasena et al., 2017; Calkin et al., 2014; Syphard et al., 2017). Specific combinations of these factors ultimately create the scenario for wildland urban interface (WUI) disasters such as the extreme Camp fire event that destroyed the town of Paradise, California (Brown, 2020) and resulted in 82 fatalities and more than 18 thousand structures lost. Similar disasters have been observed elsewhere, notably the Portugal fires in 2017 that resulted in 61 lost lives (Castellnou et al., 2018; Turco et al., 2019), and the Black Saturday disaster in 2009 resulting in 173 fatalities in southeastern Australia (Cruz et al., 2012). These events are associated with extreme and anomalous winds (Abatzoglou et al., 2018) that catalyze violent pyro-convective fire weather (Peterson et al., 2015) and ember showers (Thurston et al., 2017) that start a chain reaction of mass structure ignitions, burning entire urban subdivisions (e.g., 2018 Carr fire) and entrapping residents. Fire suppression under these severe burning conditions is minimally effective at controlling fire spread and preventing structural fires within developed areas. Top down and bottom up drivers of risk are well studied (Keeley and Syphard, 2019), including the expanding urban footprint (Radeloff et al., 2018), increasing size of community firesheds (Ager et al., 2019), increasing human ignitions (Mietkiewicz et al., 2020; Nagy et al., 2018), droughts (Littell et al., 2016), high-wind events (Abatzoglou et al., 2018), and high fuel loadings around communities (Parisien et al., 2020). Managing the human factors that contribute to wildfire disasters exceeds the capacity of existing governance systems (Charnley et al., 2020; Fischer et al., 2016; Schoennagel et al., 2017; Steelman, 2016).

Predicting wildfire disasters is a common goal for a diverse set of actors, ranging from land managers, homeowners, conservation biologists, physical scientists, and the insurance industry, but arguably there is much work to be done to improve current risk analytics. The literature on predicting extreme wildfire events includes theoretical studies (Makridakis and Taleb, 2009), and predictive modeling with meteorological explanatories as measured by burned area, under contemporary (Joseph et al., 2019; Stavros et al., 2014) or future (Stavros et al., 2014) climate. These studies predict burned area but do not predict the location of individual fire events or their impact on developed areas. Finer scale studies to predict or understand impacts of individual events on communities and surrounding developed areas can be classified into those that reconstructed exposure and loss from past fires, versus studies that used fire event simulation to predict and map future loss. The former empirical studies have examined home loss with statistical models (e.g., logistic regression, generalized linear regression) to understand how local factors such as fire intensity, fuels in the landscape versus home ignition zone, and WUI configuration contribute to structure vulnerability and loss (Alexandre et al., 2016a; Braziunas et al., 2020a; Kramer et al., 2019; Syphard and Keeley, 2019). Studies of localized conditions that directly contribute to building loss (versus exposure) have identified key relationships between loss and fuel around buildings (Bhandary and Muller, 2009; Keeley et al., 2020; Penman et al., 2019; Penman et al., 2015; Syphard et al., 2014), building construction (Syphard and Keeley, 2019; Syphard et al., 2017), and spatial arrangement and density of buildings (Alexandre et al., 2016a, 2016b; Chen and McAneney, 2004; Kramer et al., 2019; Penman et al., 2014; Syphard et al., 2012). Likewise, empirical studies that have examined the problem from larger scales have identified drivers of impacts to the built environment including landscape fuel arrangement (Gibbons et al., 2012; Price et al., 2015; Price and Bradstock, 2013a), topography (Alexandre et al., 2016a, 2016b), and fuels buildup in wildlands due to land abandonment or cessation of traditional agropastoral activities (Badia et al., 2019; Chas-Amil et al., 2020).

Fire simulation studies complement empirical approaches by filling in the gaps where fires have not occurred, providing predictive services including fine scale maps of likelihood, intensity, source, and expected building exposure from plausible, future fire events (Ager et al., 2019; Alcasena et al., 2019; Braziunas et al., 2020b; Evers et al., 2019; Haas et al., 2013). Wildfire simulation also provides an important planning framework to design and test wildland fuel management strategies (Ager et al., 2007, 2011; Riley et al., 2018) and provides insights into future extreme "black swan" events (Barclay, 2019; Donato et al., 2020; Hulse et al., 2016; Joseph et al., 2019; Taleb, 2007). Although there are many acknowledged limitations in existing fire behavior models (Cruz and Alexander, 2013), simulation methods have proven useful in a range of wildland fire research and applications (Miller and Ager, 2013; Noonan-Wright et al., 2011), especially as changes in development, fuels, and climate continue to push many fire-prone landscapes into novel vegetation states.

Despite the potential advances from combining simulation and reconstruction studies to characterize wildfire risk to developed areas, there are few if any comparative studies that attempt to merge and synthesize findings from the respective studies and methods. For example, recent investigations of the factors that contributed to structure exposure (Alexandre et al., 2016a; Kramer et al., 2019; Radeloff et al., 2018; Syphard et al., 2017) do not compare their findings to the numerous wildfire simulation studies concerned with the same general questions (Haas et al., 2013; Calkin et al., 2014; Bar Massada et al., 2009; Penman et al., 2014). This is unfortunate since synergies exist in the different experimental methods, including the extrapolation of local empirical relationships to large areas using simulation outputs. For instance, in the study of 69 wildfires in California, Kramer et al. (2019) estimated exposure and loss by WUI type and found most of the exposure and loss in the interface WUI type, with building losses ranging from 4 to 50% therein. Replicating this analysis with continental-scale simulation outputs could provide many insights into how development patterns interact with surrounding fuels in the wide range of WUI configurations as well as the diversity of fire regimes in the surrounding wildlands (Evers et al., 2019).

In this study, we provide a rare comparison between exposure predictions from empirical versus simulation modeling and examine potential future extreme wildfire events under contemporary climate. Empirical studies have described how exposure varies among discrete WUI types (intermix, interface, urban), whereas this work considers the underlying process that generates clines in exposure along the wide array of gradients of fuels and building density in areas like the western US (Fig. 1). We combine new wildfire simulation data (Short et al., 2020a) with spatially synchronized daily weather, building location data (Microsoft, 2018), and multiple sources of observational data on building exposure and loss (Alexandre et al., 2016a; Kramer et al., 2019; Mietkiewicz et al., 2020; MTBS Data Access, 2020a; St Denis et al., 2020) to examine three key questions related to the overall problem of predicting future WUI disasters: 1) How well do broad trends in simulated exposure to developed areas align with recent historical observations? 2) What is the frequency and magnitude of simulated extreme exposure events that exceed observed records? and 3) How do simulated wildfires distribute exposure among discrete WUI types used in prior studies, and how do underlying gradients in fuel and building density contribute to peak exposure? We discuss the limitations of the respective methods for studying and mapping building exposure as well as the synergies associated with the combined use of simulated and empirical exposure data to advance the global problem of predicting exposure to developed areas.

2. Materials and methods

2.1. Study area

Our study area covers the 11 western US states (Arizona, AZ; California, CA; Colorado, CO; Idaho, ID; Nevada, NV; New Mexico, NM; Montana, MT; Oregon, OR; Utah, UT; Washington, WA; and Wyoming,

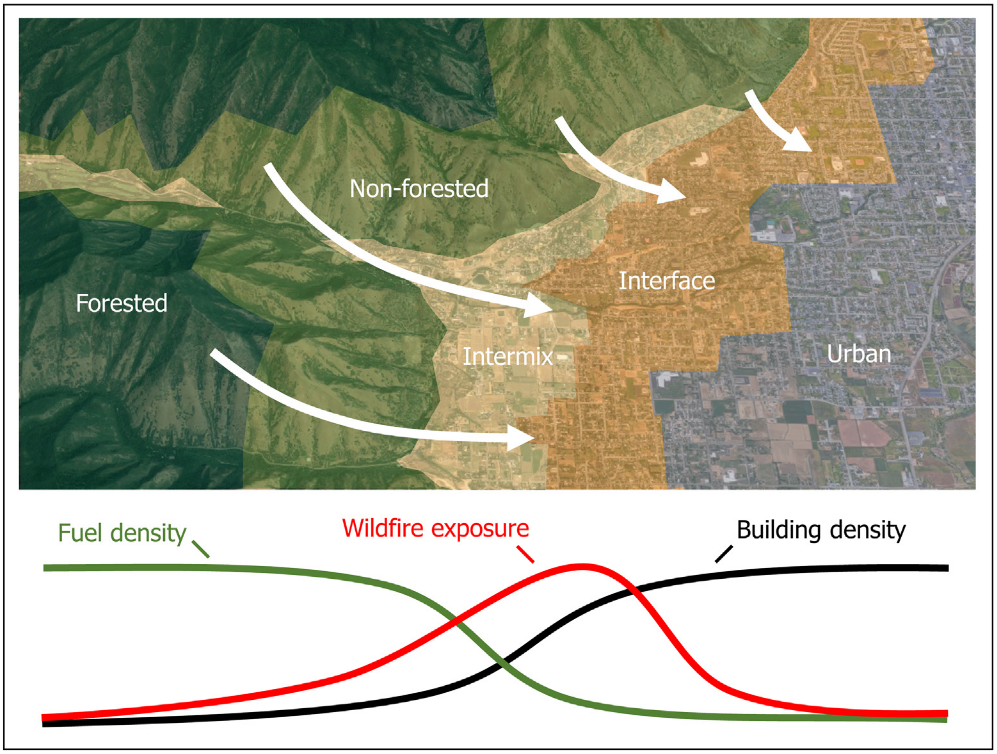

Fig. 1. Hypothetical relationship between wildfire exposure and the counter-gradients in building density and fuel density around developed areas. We hypothesized that combinations of the two optimize building exposure, a relationship that is obscured using discrete wildland urban interface (WUI) classes typically used to study WUI exposure and loss.

WY), and is about 307 million ha. It encompasses seven of the level I Omernik ecoregions (Omernik, 1987; US Environmental Protection Agency, 2019) (Appendix Fig. A1). Federal agencies manage approximately half of the landscape (145.5 million ha, 48% of all lands), and primarily include the Bureau of Land Management (BLM, 71 million ha) and the US Forest Service (FS, 57.5 million ha) (USGS, 2016). Approximately 115 million ha are fire adapted with low- and mixed-severity fires, as defined by fire regimes I (35-year fire return interval) and III (>35–200-year fire return interval). More than 65 million ha have been classified with high or very high fire potential (Dillon, 2015).

2.2. Building location data

Building locations were obtained from the vector building dataset created in 2018 by the Bing Maps team at Microsoft (2018). The data set contains over 25 million building footprints in the western US in GeoJSON format including apartments, industrial sites, housing units and storage buildings. These building data were generated from aerial images using deep learning object classification methods. We created a building centroid point file from the individual footprint polygons ($n = 25{,}402{,}440$) and used point data to predict individual building exposure from simulated wildfires as described in Section 2.4. We then converted the point file to a 30-m building count grid to analyze the effect of fuels and building density on building exposure as described in Section 2.8.2. This resulted in a grid with 5,628,979 cells containing the 25 million buildings corresponding to the 30 m burnable cell locations with at least one building footprint (Microsoft, 2018). On average each cell contained 1.09 buildings with a maximum of 8, although 92% of pixels contained only 1 building and <0.01% contained more than 5 buildings.

2.3. Burnable fuel density

The fuels layer for non-developed areas was constructed from the 30 m Scott and Burgan fuel model raster by removing all fuels types classified as non-burnable fuels including water bodies, rock/bare ground, snow, urban developed/paved, and irrigated agricultural land (LANDFIRE, 2017).

2.4. Wildfire simulation data

We used wildfire simulation data from the national FSim library (Short et al., 2020a; fire perimeters not publicly available), with 54,269,100 simulated fires for the western US. FSim consists of modules for weather generation, and for modeling large-fire occurrence, growth and suppression (Finney et al., 2011; Short et al., 2020a). The model is described in detail in prior publications (e.g., Finney et al., 2011; see also Appendix) and is widely used in the US for wildfire risk assessments at local, regional, and national scales (Dye et al., 2021; Haas et al., 2013; Scott et al., 2012; Thompson et al., 2013). In brief, FSim generates daily wildfire scenarios for tens of thousands of hypothetical contemporary wildfire seasons using relationships between historical Energy Release Component (ERC, Bradshaw et al., 1983) and historical fire occurrence. Time series analysis is used to estimate trends in daily ERC, variability, and autocorrelation, and the resulting parameters are used to simulate synthetic fire seasons with the same statistical properties of historical weather, but factor in variability in the daily average and trend (Grenfell et al., 2010) (see below). Wildfires are simulated with the minimum travel time (MTT, Finney, 2002) algorithm under weather conditions derived from the synthetic fire seasons. Resolution of the simulations in the Short et al. (2020a) library is 270 m. Fires are ignited across the landscape non-randomly using an ignition density grid derived from historical occurrence (75-km kernel density search radius and 2-km output cell size). Fire growth is predicted on days that meet threshold ERC according to empirically derived wind and fuel moisture. Fire containment is modeled with a logistic regression that predicts containment probability as a function of high versus low spread periods (Finney et al., 2009). A ‘perimeter trimming’ function is included to produce realistic fire footprints and to replicate historical fire size distributions.

For the Short et al. (2020a) products LANDFIRE data depicting fuel conditions circa 2014 were used (LANDFIRE, 2017), and fire season scenarios generated in the weather module were based on a national gridded weather dataset from the North American Land Data Assimilation System (NLDAS), which is a contemporary surface weather data assimilation system (Abatzoglou, 2013). The NLDAS data were analyzed to produce daily spatiotemporal realizations of a fire danger index (i.e., ERC) that retain the spatial covariance structure and temporal auto-correlation of the weather inputs (Grenfell et al., 2010). This approach maintains synchrony across weather scenarios used among independently simulated units. The simulation units used by Short et al. (2020a) were regions of relatively homogenous contemporary fire regimes called "pyromes" (Short et al., 2020b), with the western US comprising 67 pyromes (Appendix Fig. A2). Between 10,000 and 100,000 hypothetical fire seasons were simulated for each pyrome, depending on the historical large fire frequency. We used the first 10,000 fire season scenarios in the current analysis since all pyromes had at least 10,000 scenarios that were synchronized across all units. For the comparative analysis of simulated and historical exposure we only included fires ≥405 ha since this is the minimum fire size in the MTBS data for the western US (MTBS Data Access, 2020a). The processes of calibrating and validating FSim area burned outputs and fire-size distributions from prior CONUS simulations were presented in Finney et al. (2011), with advances described by Short et al. (2020a). For each simulated fire, we obtained the ignition location and associated perimeter for each fire as output in shapefiles, along with the burn probability raster at 270 m resolution.

2.5. Wildland urban interface

The SILVIS WUI data (SILVIS Lab, 2012) use the US Census tract polygons and provide polygon-based estimates of residential housing density where structures meet or intermingle with wildland vegetation. SILVIS data are classified according to housing density and percentage of wildland vegetation within or adjacent to housing blocks. We used four WUI categories including urban non-vegetated, intermix (housing and vegetation intermingle with ≥6.18 houses km^{-2} and >50% wildland vegetation cover), interface (housing in areas with ≥6.18 houses km^{-2} and <50% wildland vegetation but within 2.4 km of >75% wildland vegetation), and forestland (very low housing density <6.18 houses per km^2 and wildland vegetation cover ≥50%). The current data describe WUI vegetation conditions based on 2010 land cover imagery (USGS, 2011). The SILVIS data have been used in numerous prior empirical and simulation studies of wildland fire exposure (Ager et al., 2019; Radeloff et al., 2018).

2.6. Community definitions and delineation

We created community boundaries that included both core areas defined by the US Census populated places data (US Census Bureau, 2016) and the adjacent WUI as defined in SILVIS. The US Census data (US Census Bureau, 2016) identifies 5118 settlements and communities in the western US in the place names database. These communities are identified as polygons or points and map incorporated and unincorporated towns, cities, and settlements. To create a map of discrete communities that included the surrounding WUI we aggregated the core communities in the US Census data with the SILVIS WUI. We attached SILVIS WUI polygons (SILVIS Lab, 2012) to the core communities (US Census Bureau, 2016) using road networks (ESRI, 2012) and minimum travel time from the community's core to each WUI polygon. Travel speed was used to create a cost raster that was input into the Cost Allocation ArcGIS tool with a maximum distance equal to 45 min driving time. The process organized 98.3% of WUI polygons into 5132 communities, representing 65 million people and 25 million buildings as estimated by SILVIS. For specifically delineating communities (versus estimating exposure by WUI category) we removed SILVIS WUI polygons that were smaller than 0.1 ha or had building density less than two housing units per km^2, thus our definition of WUI includes lower density census blocks than Radeloff et al. (2005) and includes no thresholds for wildland vegetation.

2.7. Historical wildfire area burned and building exposure

Historical data on area burned and building exposure were obtained from multiple sources (Table 1) and used in several comparisons as detailed in Section 2.8. Annual area burned for 1984–2018 and historical fire footprints for 1990–2018 were obtained from MTBS (MTBS Data Access, 2020a; MTBS Data Access, 2020b) and include fires ≥405 ha but exclude prescribed fire and "unknown" fire type boundaries. Data on observed annual building exposure were obtained from several case study publications and published data sources (Table 1).

Table 1
Summary of data and analyses used for each of the major questions in the study.

Question	Data sources
1. Do broad trends in simulated exposure to developed areas align with recent historical observations?	a) Observed area burned: MTBS fire occurrence data 1984–2018 (MTBS Data Access, 2020b) b) Simulated area burned: FSim simulation outputs (Short et al., 2020a; fire perimeters not publicly available). c) Observed building exposure: MTBS perimeters 1990–2018 (MTBS Data Access, 2020a) intersected with MS building data from 2015 (Microsoft, 2018) and summarized by Omernik Level 1 ecoregion (US Environmental Protection Agency, 2019) and compared with Alexandre et al. (2016a) and simulated building exposure d) Simulated building exposure: FSim perimeters (Short et al., 2020a) intersected with MS building data from 2015 (Microsoft, 2018) and summarized by Omernik Level 1 ecoregion (US Environmental Protection Agency, 2019)
2. What is the frequency and magnitude of simulated extreme exposure events that exceed observed records?	a) FSim outputs screened for extreme fire years and individual fire events for area burned and building exposure b) Exceedance probabilities (Feller, 1968) calculated for each community as defined in Ager et al. (2019) and by Omernik Level 1 ecoregion (US Environmental Protection Agency, 2019) using FSim perimeters (Short et al., 2020a) intersected with MS building data (Microsoft, 2018) c) Simulated exposure regimes (exposure frequency versus magnitude) compared among 5132 communities
3. How do simulated wildfires distribute exposure among the discrete WUI types used in prior studies, and how do underlying gradients in fuel and building density contribute to peak exposure?	a) FSim perimeters intersected with SILVIS WUI data (SILVIS Lab, 2012) and compared with Kramer et al. (2019). b) Burnable fuel density (LANDFIRE, 2017) and building density were used to estimate building exposure from MS footprint data (Microsoft, 2018) and FSim outputs (Short et al., 2020a)

2.8. Analysis

2.8.1. Comparison of observed and simulated exposure

The analyses for the specific questions in the study are outlined in Table 1. We used multiple data sources to obtain and compare estimates of historical and simulated building exposure to gain insights into how exposure from simulation modeling compares to historical observations. We calculated annual area burned from simulation outputs by summing the total area burned by fre season for the 10,000 simulated fire seasons after filtering for fires ≥405 ha to match historical data from MTBS. Fires smaller than this size contribute a minimum amount to total area burned in the West. These comparisons served to validate simulation outputs in terms of burned area from the newer FSim simulations (Short et al., 2020a). Simulated fire perimeters were intersected with the MS building footprints to estimate annual building exposure and create frequency distributions of exposure by fire season scenario for the western US. The western US estimates were compared with observed exposure obtained from MTBS fire perimeters.

We then conducted a finer scale comparison using historical and simulated wildfire exposure at the intersection of WUI class (forestland, intermix, interface, urban) and within the seven ecoregions using historical data and simulation outputs. Here, we partitioned the exposure data from simulations by WUI class and ecoregion, and calculated averages in terms of both total building count and percentage of total buildings exposed. To permit comparison with prior research (i.e., historical data) we did these calculations using two sources of building location data, the first being the SILVIS density values attached to each WUI polygon, the second being the MS building footprint data. We then estimated historical exposure by intersecting the MS building footprint data with the MTBS perimeters and performed the same calculations. Finally, we compared the above estimates of exposure with the tabular data presented in Alexandre et al. (2016a) for exposure by ecoregion for fires >405 ha for the period 2000 to 2010, and Kramer et al. (2018) exposure by WUI class for 69 selected wildfires in California for the period 2000 to 2013 (Table 1).

Exceedance probability (EP) graphs were calculated to quantify the relationship between probability and exposure level at the ecoregion and community scale. EP is the probability that a certain value will be exceeded in a predefined future time period (Feller, 1968). EPs are widely used in the natural disaster field as part of risk and hazard assessments for floods, earthquakes, and hurricanes (Lambert et al., 1994; Mills et al., 2018; Sajjad et al., 2020). EP graphs that estimate financial losses (instead of building exposure, for instance) are the basis upon which insurers estimate the likelihood of experiencing various levels of loss and the appropriate premiums. For example, for the 10,000 simulated fire season scenarios the highest exposure season will have a 0.01% chance of being exceeded. This is because there is only one event with a loss greater than or equal to that loss in 10,000 years of events ($1/10{,}000 * 100 = 0.01\%$). The inverse of the EP is the contemporary annualized probability for an event that exceeds a given magnitude.

EP graphs were generated by intersecting fire perimeter shapefiles with MS building footprint centroids and then aggregating the count of exposed buildings by year. The count of buildings exposed per year was then sorted in descending order and the EP (probability of higher exposure) calculated for each interval. We calculated EPs for both total building exposure and as a percentage of the total to highlight regions that had higher probability of building exposure but relatively fewer buildings.

EPs by community were estimated by attributing communities with the total number of buildings and intersecting communities with FSim wildfire perimeters. Yearly building exposure for each community was summarized as well as the percentage of buildings exposed by year. These data were used first to examine the number of communities that would experience a given level of exposure each year at six EP levels, and compare the variation around each exposure level as shown by box plots. In this way, the expected number of communities impacted at a specific level of exposure could be estimated. We created EPs using both the percentage of the buildings in a community and the total buildings to understand extreme events at the scale of individual communities, to understand relative versus absolute exposure at the community scale. By analyzing the percentage exposed we were able to highlight small but highly exposed communities (e.g., Paradise, CA) according to simulations. We then created maps of EPs for four levels of exposure.

2.8.2. Effect of fuels and building density on simulated building exposure

We used data for building density (Section 2.2), fuels density (Section 2.3), and burn probability (Section 2.4) to test the hypothesis that specific combined values of these variables maximize building exposure as described at the outset of the paper. Smoothed grids for each of the three variables were used to obtain average estimates per 1 km^2 area circle using nearest neighbor resampling. Simulated building exposure per km^2 was the product of the building density and burn probability. Annual building exposure per km^2 was then estimated with the model:

$$Exp = s(BD, BurnP) + ecoregion + error \quad (1)$$

where *BD* is the number of buildings within a 1 km^2 circle, *BurnP* is the burnable fuel proportion within a 1 km^2 circle ranging from 0 to 1, *ecoregion* is a categorical variable indicating the Omernik ecoregion (sensu Alexandre et al., 2016a), $s()$ is a two dimensional smooth spline function and *error* is random Gaussian noise. The model was estimated using generalized additive models (GAM) with the Mixed GAM Computation Vehicle (mgcv) package in the open source R statistical package (R Core Team, 2019).

3. Results

3.1. How well do broad trends in simulated exposure to developed areas align with recent historical observations?

Observed annual area burned in the western US was 1.19 million ha for the period 1990–2018, compared to 1.21 million ha from simulations (Table 2, Fig. 2A). Observed annual building exposure obtained from intersecting fire event perimeters and MS building footprints from 2000 to 2018 was 10,080 buildings (Table 2, Fig. 2B). Building exposure from

Table 2
Summary of estimates for area burned and building exposure from observed and simulation outputs. See Table 1 and text for additional details.

Attribute	Simulated	Observed
Number of fire seasons	10,000 replicate fire seasons	29 (1990–2018)[a]
Mean annual building exposure	23,139	8898[b]
Mean annual area burned (ha)	1,213,438	1,185,748
Extreme year area burned (ha)	8,260,639 (replicate = 7057)	2,968,379 (year = 2012)[c]
Extreme year building exposure	495,843 (replicate = 9338)	39,505 (year = 2018)

[a] Comparisons by ecoregion included 19 fire seasons (2000-2018) to align with other published studies; annual area burned metrics included 35 fire seasons (1984-2018) for the histogram in Fig. 2.
[b] The observed average exposure (23,302 buildings) in only the last 3 years of the analysis (2016 to 2018) was equivalent to simulated exposure as noted in the table.
[c] Note that preliminary numbers on area burned for the 2020 fire season in the western US are estimated to be approximately 1.2× higher.

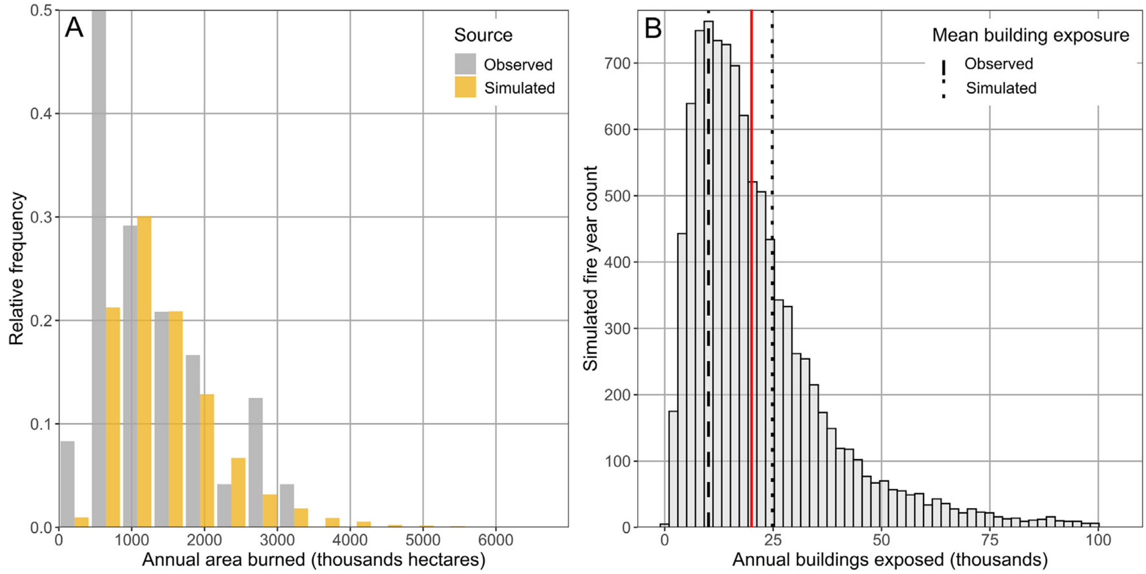

Fig. 2. Probability distributions for area burned (A) and buildings exposed to wildfire (B) for recent historical and simulated fire events. Panel A is truncated at 700,000 ha (excludes two bins for simulated data only with probability <0.0003). Panel B is truncated to 100,000 buildings (125 years simulated >100,000 buildings exposed). Data sources and date ranges are in Table 1. The Camp fire that burned most of Paradise, CA is shown as a red line; data are based on CalFire (2020).

simulated fires was substantially higher at 23,139 buildings per year (Fig. 2B). However, when the observed building exposure was calculated for the last 5 years of available data (2014–2018), the value increased to 17,280, or within 75% of simulated (Appendix Fig. A3), and for the last three years of data within 94%. Annual variation in building exposure as measured by standard devaition (Appendix Fig. A3) for the same five years was 14,851 buildings.

At a finer ecoregional scale, comparing observed (MTBS perimeter and MS building data) and simulated (FSim perimeter and building data) wildfires revealed variable differences (Fig. 3; Appendix Table A1). In some ecoregions the observed and simulated were similar (Great Plains (GPL) and Mediterranean California (MCA)) while other

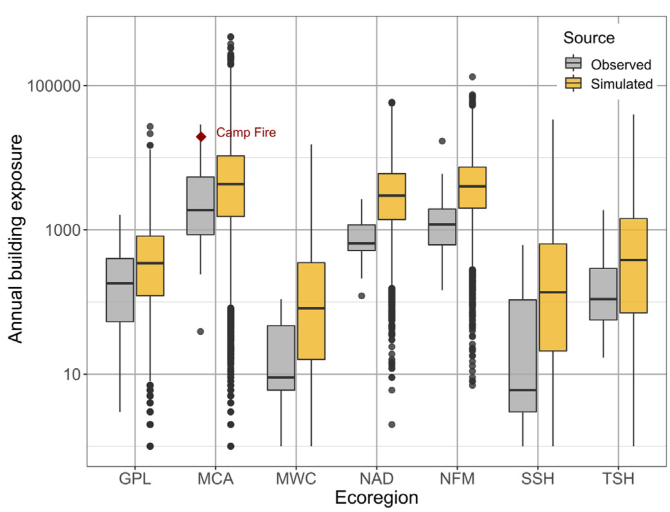

Fig. 3. Boxplots of annual building exposure calculated from observed MTBS (2000–2018) (MTBS Data Access, 2020a) and simulated FSim wildfire perimeters (10,000 fire season scenarios) intersected with MS building footprints. Note log scale on the y-axis. The 2018 Camp fire is shown for reference with the number of exposed buildings according to CalFire (2020) (19,558). Black box lines are medians, the tops and bottom of the boxes are the 75th and 25th percentiles, whiskers represent 1.5 times the low and high percentiles; outlier data points outside the whiskers are denoted by dots. GPL = Great Plains, MCA = Mediterranean California, MWC = Marine West Coast Forest, NAD = North American Desert, NFM = Northwest Forested Mountains, SSH = Southern Semiarid Highlands, TSH = Temperate Sierras.

regions exhibited larger differences (North American Desert (NAD) and Northwest Forested Mountains (NFM)). Interestingly, the range of values between the 25th and 75th percentiles in the respective data sources had substantial overlap (Fig. 3, vertical range of boxes), although the simulation data contained substantially more outliers which was expected given the larger sample size (10,000 versus 19).

The comparison between total observed and simulated exposure by ecoregion is expanded in Fig. 4 to include multiple sources of observed data. The magnitude of the overprediction estimated with the same data as in Fig. 3 was concentrated in two of the ecoregions (NAD, NFM). Both observed and simulated exposure were highest for the MCA ecoregion by over twice the value as the next highest region (Fig. 4A). The highest underprediction between observed and simulated corresponded to the GPL where modeled values were 5 to 6 times lower. Simulated exposure was on average about 20% higher when using the FSim-MS building data (building data vintage = 2015) compared to FSim-SILVIS WUI census block data (housing unit data vintage = 2010) (Fig. 4A). The distribution of exposure among the ecoregions expressed as a percentage of the total exposure within each data set was similar as measured by the FSim-SILVIS or FSim-MS building data (Fig. 4B). Simulated exposure on a percentage basis was spread more evenly among the ecoregions compared to observed obtained from prior studies and historical data. Although total building exposure estimated from simulation was substantially higher when calculated with the FSim-MS building data compared to FSim-SILVIS (Fig. 4A), as a percentage of total buildings exposed the two data sets provided similar results (Fig. 4B). In other words, the simulation estimates were proportionately lower in MCA, and higher in all the other ecoregions except the GPL, compared to observed. Comparing the two observed data sources (Alexandre et al. (2016a) and the MTBS-MS building), we note that estimates are similar except for a higher exposure in the NFM ecoregion based on MTBS-MS building, and higher exposure in GPL based on Alexandre et al. (2016a).

3.2. What are is frequency and magnitude of simulated extreme exposure events that exceed observed records?

3.2.1. Western US

In terms of extreme fire years included in this study (1990–2018) in the western US, the largest burned area between was in 2012

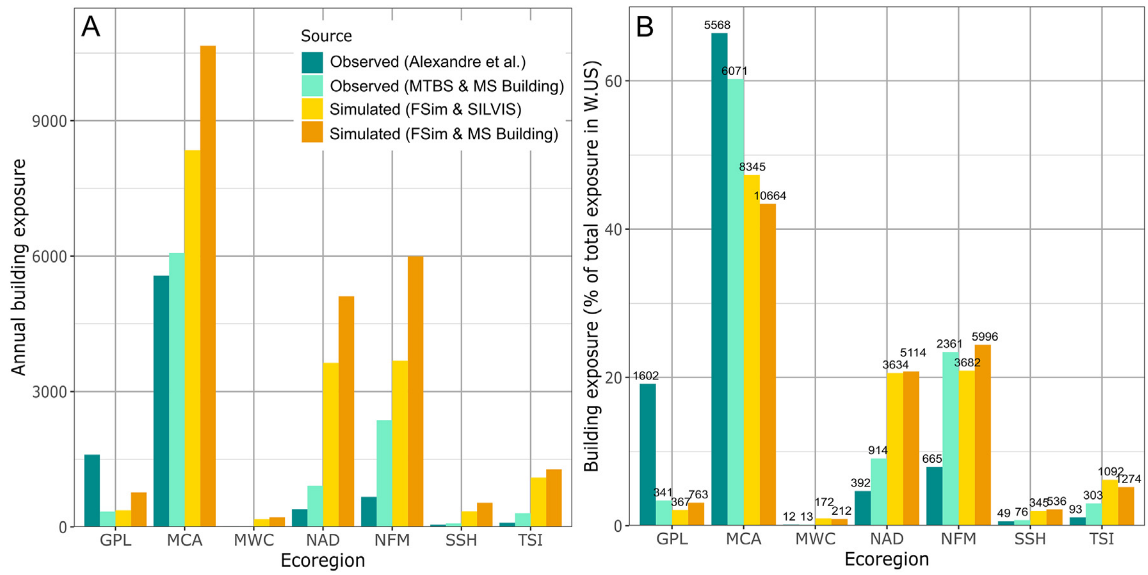

Fig. 4. Comparison of observed and simulated building exposure from wildfires in the western US by ecoregion. (A) Annual number of buildings exposed, and (B) percentage of total by ecoregion for each data set. The data include: (1) empirical observations from Alexandre et al. (2016a) where all buildings, exposed and lost, were manually digitized for large fires (>405 ha) occurring during 11 years (2000 to 2010); (2) estimates from intersecting MTBS perimeters with MS building data; (3) simulated data derived from intersecting SILVIS WUI polygons (Martinuzzi et al., 2015) and FSim perimeters; and (4) intersection of MS building data with FSim fire perimeters (Table 1). Definitions for the ecoregions are in Fig. 3.

(2,968,379 ha), compared with a simulated fire year that burned 8,260,639 ha in 1782 fires, exposing 76,210 buildings within the perimeters (Appendix Fig. A4; we note that preliminary data on the 2020 fire season showed an even higher area burned–3.6 million ha resulting in 46 fatalities, and 13,887 buildings lost– although the lack of fire perimeters precluded inclusion in this study). The largest number of buildings exposed in a single simulated year was 495,843, when 3,964,265 ha burned in 436 fires (Appendix Fig. A4A). Given there are 10,000 simulated fire seasons, this extreme year has a probability of 1 in 10,000. The worst observed fire year in terms of buildings exposed or burned was 39,505 buildings in 2018 (Appendix Fig. A4B). The most extreme exposure event from a single simulated fire was 106,378 buildings in California in a fire that burned 470,578 ha. The maximum number of observed buildings exposed was 16,855 from the 2018 Camp fire, as estimated from the intersection with MTBS perimeters and Microsoft building data (19,558 structures according to CalFire (2020); Appendix Fig. A5).

3.2.2. Ecoregions

Ecoregional extreme events were quantified with EP graphs that show the probability that a certain exposure threshold will be exceeded by ecoregion per year. The high levels of exposure in the Mediterranean California ecoregion evident in the prior results are reflected in the EP graph where for instance there is a 1% probability that more than 150,000 buildings will be exposed to fires per year (Fig. 5A). By contrast,

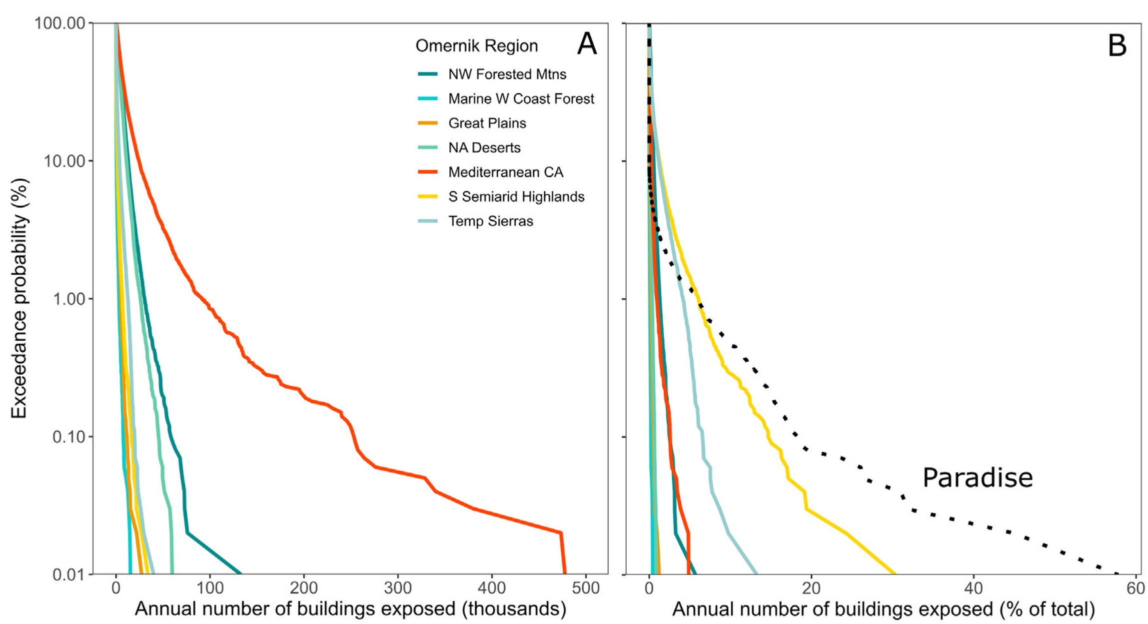

Fig. 5. Exceedance probabilities (EP) for the western US by ecoregion showing the probability of annual building exposure being exceeded by a specified level. EP of (A) total building exposure in a given year; and (B) as a percent of total buildings in the ecoregion. The EP for Paradise (in the Mediterranean CA ecoregion) was derived from the simulation library of fire perimeters that were intersected with the buildings in that specific community using fuels data that preceded the 2018 Camp fire.

the Northwest Forested Mountains, which had the next highest probability of extreme events, showed much lower exposure relative to Mediterranean California, and the lack of extreme, low probability events in all the regions was evident (Fig. 5A). However, when expressed as a percentage of total buildings in the ecoregion (Fig. 5B), the simulated exposure was higher for other regions, particularly in the Southern Semiarid Highlands, and North American Desert regions (Fig. 5B). The comparison of total exposure to per building exposure highlights relative risk to individual buildings versus populations of buildings in developed areas. This comparison highlights the relative effects of building density versus fire frequency as the cause of exposure. The shifting of the EPs among the regions between total and per building exposure shows (Fig. 5A versus B) that high exposure in Mediterranean California results from a large number of buildings and that the probability of exposure for a given building is actually higher in most of the other ecoregions. Interestingly, the EP for Paradise, California, derived from the simulations on a per building basis prior to the 2018 Camp fire, was substantially higher than all the ecoregional estimates (Fig. 5B).

3.2.3. Communities

Box plots show the total number of communities in the western US exposed to wildfire as measured by the percentage of buildings in the community that fall within a fire perimeter in simulation (Appendix Fig. A6). In any given year, the simulations indicate that about 25 communities had at least 5% of the buildings exposed to fire, and about four communities had at least 50% of the buildings exposed. The median number of communities where 100% of the buildings were exposed was near 0. Box plots show large variation around the median number of communities for low levels of exceedance. At the 5% exceedance level the difference between the 25th and 75th percentiles ranged from a low of 18 to a high of 39 communities.

Mapping EP by community (Fig. 6) pointed to several hotspots of simulated exposure as measured by the percentage of buildings exposed annually. At the highest exposure level, hot spots are evident in northern NV, north central UT, southern CA and southern NM. Contrasting the four panels (5%, 25%, 75%, and 95%) shows regions of higher probability of exceedance at low levels, versus lower probability of exposure at high exceedance levels, meaning that the shape of the EP relationship changed among the communities. Thus, some regions had a high EP for a low impact event (e.g., southwest Oregon, Fig. 6) but a relatively lower EP for a higher impact event, in comparison to other areas (e.g., central UT). Paradise, California had an EP of 0 for exceeding both 75% and 100% building exposure (0.0001 for EP of 50%). Mapping EP by total building loss (Appendix Fig. A7) generally highlighted communities in California and Arizona as indicated in other results.

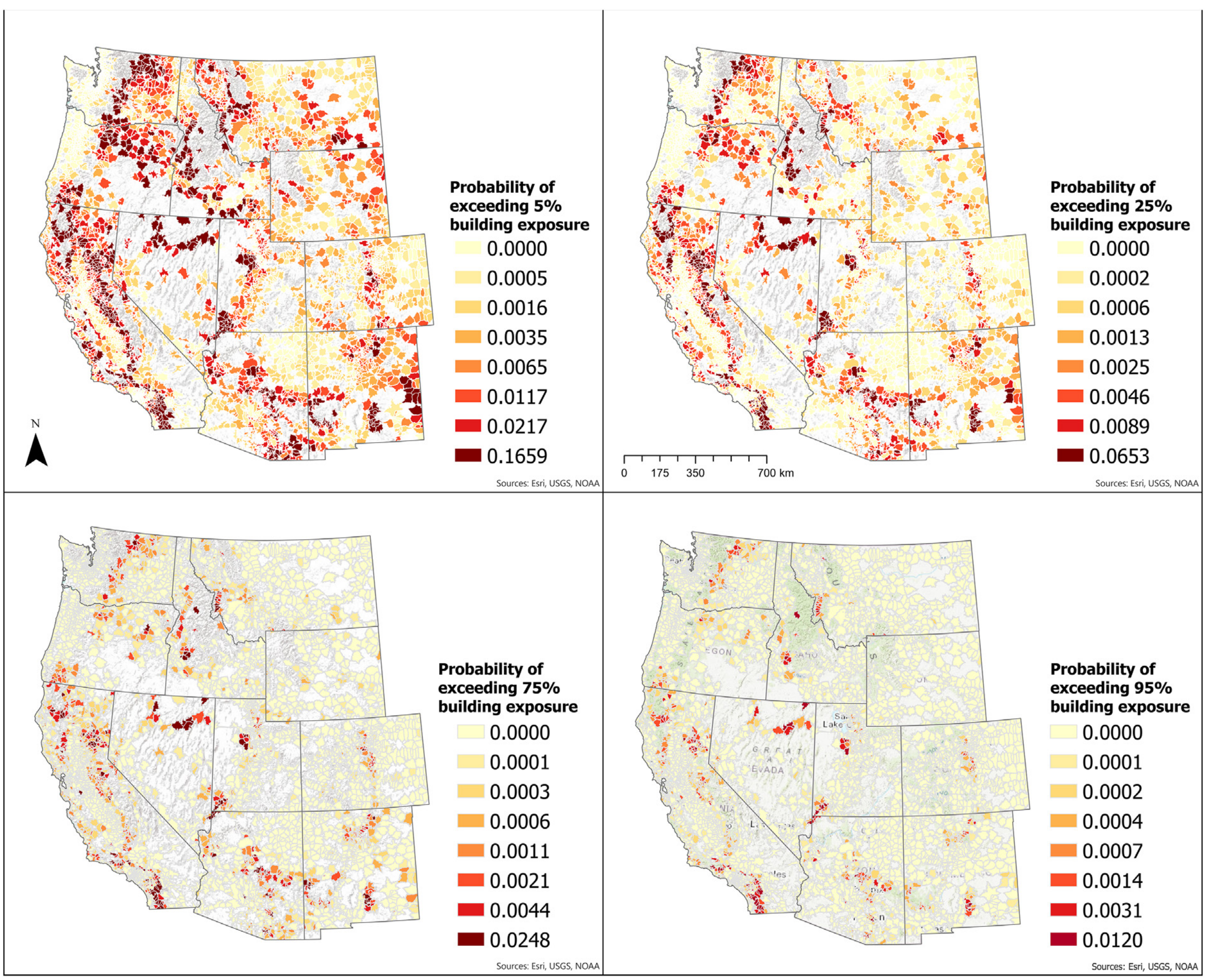

Fig. 6. Exceedance probabilities (EP) maps for four levels of community exposure in the western US expressed as the percentage of buildings exposed. Building exposure was estimated at the community scale for 5132 communities. Images show EPs for 5%, 25%, 75%, and 95% of total buildings exposed within a community in a given year. Fig. A7 in the Appendix further highlights variation in exposure regimes, i.e. the frequency versus intensity of exposure events for individual communities (*sensu* fire regime, (Morgan et al., 2001). The relationship between low and high impact events for a particular community was correlated for extreme values in terms of the number of buildings exposed (Appendix Fig. A8), although there were many outliers where there was a relatively high probability of exceeding a single building exposed, but close to zero probability of a high impact event. Conversely there were many communities that had only high probability events if an event occurred. Overall, simulation outputs predicted widely different fire exposure regimes among the communities in the study area.

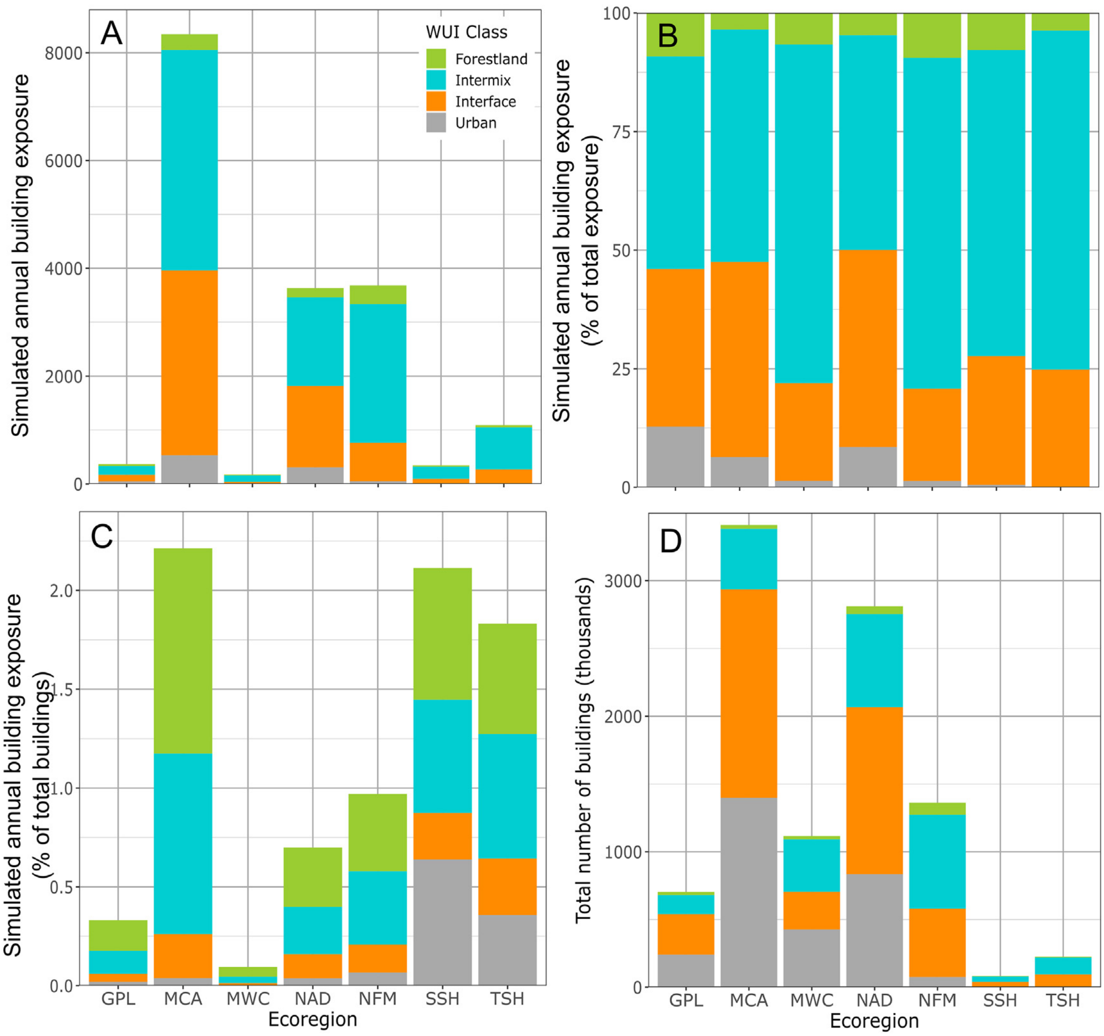

Fig. 7. Simulated building exposure by ecoregion and wildland urban interface (WUI) class using SILVIS housing density data and wildfire simulation perimeters. (A) Simulated total annual building exposure by WUI class and ecoregion, (B) percentage of total building exposure within each ecoregion by WUI class, (C) exposure by WUI class expressed as a percentage of the total buildings in that ecoregion, (D) total number of buildings in each WUI class as derived from SILVIS. Definitions for the ecoregions are in Fig. 3. See Appendix A Table A2 for exposure by WUI class and housing density class.

3.3. How do simulated wildfires distribute exposure among WUI types and what are the relative effects of fuel versus building density?

Interface and intermix WUI accounted for the vast bulk of the simulated exposure in all ecoregions, while urban and forested categories accounted for the least (Fig. 7A, B). While interface was a substantial WUI type in terms of total and percentage of total exposure at the ecoregional scale (Fig. 7A, B), on a per building basis they were marginally exposed compared to the other WUI classes (Fig. 7C). In terms of the relative likelihood of exposure on a per building basis, forested areas went from the lowest to the highest (Fig. 7C). This finding indicates that the high exposure in the interface results from a relatively large number of buildings (Fig. 7D), and the high exposure in the intermix results from more fire exposure per building. Our results for the Mediterranean California (MCA) ecoregion were similar to Kramer et al. (2019) for interface and non-urban WUI classes (Appendix A Table A4), but higher for intermix (49% with simulation versus 37.6% observed), and lower for Non-WUI, rural.

Results from the GAM modeling of the 25 million building observations in the western US showed the compensating effects of building density and burnable fuel on simulated exposure, meaning that conditions that reduced exposure in one of the variables could be increased by changing the value of the other (Fig. 8A). The results suggested peak exposure at a fuel density of 0.7 and a building density between 1400 and 1500, although the region of high exposure was broadly defined by the two explanatory variables. These same patterns were evident for all ecoregions, however the estimated exposure values were lower by a range of −0.0015 to −0.008 for the remaining ecoregions (Appendix A Table A3).

We created five hypothetical wildfire spread scenarios that start in the wildlands (e.g. left, Fig. 1, upper left Fig. 8A) and transitioned through increasing building density and decreasing fuels (Right, Fig. 1, lower right Fig. 8A). These gradients typify the spread patterns of large fires (e.g., Carr fire) that start in wildlands and spread to developed areas through increasing density of buildings. Exposure values were then estimated from the GAM model along the scenarios and plotted at equal intervals in relation to building and fuels density (Fig. 8B). The results showed that each scenario had a slightly different maximum exposure in relation to fuel density, mostly in the region of 0.4 to 0.6. Scenarios where fires passed through higher fuel and building density showed maximum exposure at the higher levels of the two explanatories, as illustrated in the shifting of the peak to the right in Fig. 8A. At lower levels of fuel and building density (scenarios at the lower left

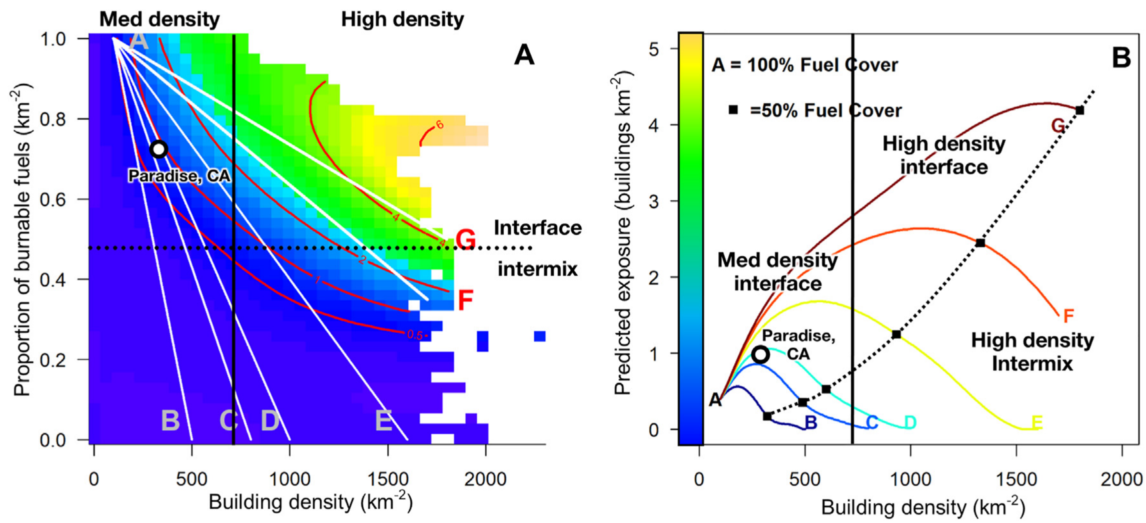

Fig. 8. Relative effect of building versus fuel density on simulated building exposure for the Mediterranean California ecoregion. (A) Isolines estimated with the generalized additive models procedure as outlined in the methods show building exposure per km^2 with hypothetical transects from the wildlands to developed areas for reference in panel B with comparison of SILVIS wildland urban interface (WUI) classes. (B) Simulated exposure for hypothetical transects shown in A show the existence of peak values of building exposure. Paradise, California is noted in both panels for reference. Black vertical lines indicate the threshold for medium versus high density WUI. Note that very low and low density WUI classes (<49.42 structures km^{-2}) are not shown and the definition of interface includes distance to wildland vegetation not considered here.

side of Fig. 8A), there was little evidence of a specific combination of fuels and buildings that maximized simulated exposure.

4. Discussion

We described potential extreme wildfire events at multiple scales in the western US and examined how gradients in fuels and buildings contribute to exposure. The study was motivated by the Camp fire and the resulting disaster in Paradise, California, and whether the likely locations of future events of similar magnitude can be mapped with simulation modeling. The results of the study have widespread application for: 1) the design of future peri-urban developments that avoid specific fuel/building densities that maximize exposure; 2) disaster planning for potential future black swan fire events and seasons (Barclay, 2019; Hulse et al., 2016; Joseph et al., 2019); and 3) prioritizing federal assistance to high exposure communities similar to Paradise, California.

While many empirical studies of WUI exposure focus on extreme wildfire events, most simulated risk and exposure assessments in the US and elsewhere (Ager et al., 2019; Bar Massada et al., 2009; Oliveira et al., 2020; Scott et al., 2013) do not, rather they report expectations of average impacts from fire events. Given predicted climate change effects on the global fire footprint (Abatzoglou and Williams, 2016; Abatzoglou et al., 2019; Liu et al., 2010), analytical templates need to begin incorporating the assessment of wildfire exposure from extreme wildfire events as with other natural disasters. As noted in the introduction, despite the potential contributions from both predictive and empirical reconstruction studies to understanding the WUI wildfire problem, most of the recent empirical studies (Alexandre et al., 2016a; Kramer et al., 2019) have not compared their findings relative to the numerous wildfire simulation studies to understand exposure and loss (e.g., Bar Massada et al., 2009; Oliveira et al., 2020; Penman et al., 2014; Calkin et al., 2010; Haas et al., 2013) and the effects of fuel treatments (Ager et al., 2007; Penman et al., 2015).

Simulation models are widely used in disaster and hazard prediction, including hurricanes and earthquakes (Irikura and Miyake, 2011; Vickery et al., 2000), and when carefully interpreted on a background of empirical data can provide predictive capabilities not afforded in empirical studies of past events. Conversely, empirical studies can describe and validate complex interactions between wildfires and building characteristics (Maranghides and Mell, 2011; Syphard et al., 2017) that contribute to loss (versus exposure) that have yet to be incorporated into large fire event simulation systems. Our study focused on the probability and intensity of exposure from future events rather than identifying explanatories for exposure from events that already occurred. While empirical data sets are becoming larger with each disaster, extrapolation to unaffected areas still lacks sufficient sample size to map risk at a scale that is useful for prioritizing and designing strategic fuel management projects, and to distinguish communities at risk from different types of fire regimes, either from chronic low impact fire or infrequent highly destructive events. Although there are other methods for predicting exposure and loss from empirical data (e.g., Syphard et al., 2019), these are difficult to scale up over broad regions, and less efficient given the national wildfire simulation library (Short et al., 2020a) and the availability of landscape fire models and associated data (Brittain, 2015; LANDFIRE, 2014).

Our study examined three interrelated questions concerning future wildfire impacts to developed areas in the western US as follows.

4.1. How well do broad trends in simulated exposure to developed areas align with recent historical observations?

Simulation estimates of exposure were compared with multiple sources of empirical data at multiple scales to understand the predictive capabilities of modeled wildfires. Total annual simulated exposure for a single extreme wildfire event the western US was significantly higher (2.6 times) than observed exposure, despite the fact that simulated total area burned in simulation was within 2% of the observed. The overprediction of exposure in terms of absolute numbers of total buildings was primarily concentrated in three ecoregions (Mediterranean California, North American Deserts, and Northwest Forested Mountains) and was on average about 20% higher when using the MS building data compared to SILVIS WUI. In general, the simulation estimates were spread more broadly among the ecoregions compared to the empirical which were heavily concentrated in the Mediterranean California ecoregion. However, the historical record is limited ($n = 19$) and highly variable over the time period used (Appendix Fig. A3). One explanation is that increased fire suppression effort and expenditures and resulting containment resources specifically for WUI fires (Clark et al., 2016; Gude et al., 2013) are effective at containing spread into developed areas, whereas the FSim containment model which uses daily trends in ERC to predict the probability of containment (Finney et al., 2011) is blind to fire spread into the WUI. We also did not specifically model increased suppression resources that are deployed in and around communities during wildfire events and potentially halt the progression of fires (Gude et al., 2013). For example, the 2018 Camp fire failed to reach the suburban community of Chico as a result of fire suppression efforts (Brown, 2020) (33,931 MS building footprints in Chico). Simulated wildfires were suppressed according to historical relationships between suppression success and daily trends in ERC (Finney et al., 2011), and burned only where there were combustible wildland fuels as indicated by LANDFIRE data.

4.2. What is the frequency and magnitude of simulated extreme exposure events that exceed observed records?

At both the ecoregional and community scale we expected and found large differences in both total and per building estimated exposure as evidenced in EP graphs. However, assessing exposure as a percentage versus total buildings exposed changed the relative ranking substantially (Fig. 5, Appendix Fig. A8). Not surprisingly, communities in southern California with relatively large urban sprawl over extensive areas nestled in fire prone vegetation dominated the highest ranked communities in terms of total building exposure. However, on a percentage of total buildings in a community, we identified smaller rural communities scattered throughout the study area with high exposure, especially ones that were surrounded by extensive national forest lands. While total exposure is a useful prediction for large scale disasters, from a community resiliency standpoint (Kulig and Botey, 2016; Norris et al., 2008), we suggest that community resiliency is lower for small communities that face extreme loss (e.g., 100%) versus large communities that face minor losses (e.g., <1%) even though total affected buildings is equal.

Our results showed the wide spectrum of exposure regimes for communities in the western US and that frequency and magnitude of exposure are community scale properties. The wide range of community exposure regimes in terms of frequent-low exposure versus infrequent high exposure events is a parallel concept to natural fire regimes (Barrett et al., 2010). Community exposure regimes arise from local variation in the natural and human driven fire regimes of the surrounding wildlands as determined by ignition frequency, fire spread rates, fuels and the spatial building patterns that determine the permeability of the community to fire (Syphard et al., 2017). For instance, communities with a high proportion of burnable fuels are more susceptible to high exposure events, and those surrounded by high frequency fire regimes are also exposed to frequent fire. In general, larger communities where a significant area is in non-burnable conditions in part explains differences in exposure regime either per building or in terms of total exposure. Communities such as Paradise, California, that are surrounded by a high frequency natural fire regime and have high permeability to fire based on building density and fuels, are more susceptible to extreme exposure events. Recent wildfire seasons indicate that building exposure regimes are rapidly changing just as ecological fire regimes are as well (Cansler and McKenzie, 2014; O'Connor et al., 2014). Community fire regimes are a potentially useful classification to communicate and tailor community-specific actions to protect against fire and measure community adaptation to fire as a local disturbance. For instance, chronic low intensity fires are an ignition prevention problem, rather than building arrangement and urban fuels, and communities are more likely to adapt to this type of fire regime (Toman et al., 2014). Conversely, communities faced with infrequent, large fire events and resulting extreme exposure will face a significantly more difficult process for community adaptation and effective protection.

Risk assessment case studies in the US and elsewhere describe long run average expectations largely derived from simulation that do not reflect rare black swan (Taleb, 2007) or extreme wildfire events (Attiwill and Adams, 2013; Tedim et al., 2018; Viegas, 2013) that drive changes in ecosystems and their fire regimes (Coop et al., 2020). Although these events are associated with the tails of the fire exposure distributions, where errors can be large, identifying the intersection of communities and these extreme events is informative. Large fires have a proportionately larger impact on ecosystems and people (Tedim et al., 2018). Studies suggest that over time, if extreme events (e.g., "gigafire", Gabbert, 2020) become more frequent, eventually fire-on-fire feedbacks self-limit burned area (Parks et al., 2016; Prichard et al., 2017). However, vegetation type changes that can result from increasingly high intensity fires and a changing climate (Stephens et al., 2013) can accelerate fire return intervals, facilitated by increases in human ignitions (Mietkiewicz et al., 2020). This trend was observed in a forest modeling study where over a 50-year time period, fire feedbacks were initially negative and turned positive as the landscape became dominated by early successional vegetation with higher rates of spread (Ager et al., 2017). Colonization of frequently burned landscapes by invasive species can further accelerate reduction in fire return intervals (Kerns et al., 2020).

In-practice, traditional risk models may be improved by considering hazard, vulnerability, resilience, and extreme events. This broader approach will help prioritize longer term outcomes to reduce vulnerabilities, as well as strengthen community resilience for risk mitigation and adaptation to future hazards, which is also stressed in the Sendai Framework for Disaster Risk Reduction adopted by the United Nations (2015). A comparatively new risk assessment narrative has been discussed that considers both natural hazard potential and resilience of communities (Angeler et al., 2018; Sajjad and Chan, 2019). It is possible that simulation modeling as employed in risk analysis can contribute in multiple ways to understanding community variation in terms of both adaptive capacity and resiliency. As discussed above, fire adaptation as an ecological process occurs as frequent fire selects for fire adapted species, just as frequent, low intensity exposure will lead to homeowner fire adaptation at the community scale (Ghasemi et al., 2020), although see Martin et al. (2009). To our knowledge, studies of risk perception (Fischer et al., 2014) have not examined how the process of adapting to wildfire would proceed down different pathways for different exposure regimes. Likewise, we suggest communities that have the potential for near 100% exposure from infrequent fires (Fig. 6, lower right) would have lower resiliency than those exposed to higher frequency low impact events.

4.3. How do simulated wildfires distribute exposure among the discrete WUI types and what are the relative effects of fuel versus building density?

At the resolution of individual SILVIS WUI classes, simulated exposure was highest for interface and intermix as observed in prior studies. The results suggested that high exposure in the former is due to the absolute number of buildings, while in the latter it stems from higher burned area. Relative exposure among WUI classes reported by Kramer et al. (2019) for the Mediterranean California region was similar, with our simulated exposure higher in the intermix (49% versus 37.6%). Kramer et al. (2019) also reported much lower exposure in the Non-WUI, rural compared to simulation (13.5 versus 3.5%) (Appendix Table A4). The bulk of the buildings and observed absolute exposure in the Kramer et al. (2019) study were in the interface, but comparisons are coarse given our results were specifically for the Mediterranean California ecoregion.

Results from the GAM modeling disentangled the different exposure regimes associated with specific WUI classes (Fig. 8) into a gradient of exposure with compensatory effects of building density and wildland fuels. We found that building exposure can be high in the intermix or interface depending on the burnable fuel fraction and building density (Figs. 1, 8). Thus, high levels of per building exposure are possible in any of the WUI classes, conditional on specific combinations of burnable fuels and buildings. Paradise, CA fell within the upper margin of the plot at a fuel density of 0.7 and building density of 314 km^{-2} (Fig. 8; note that Paradise is considered majority intermix based on 2010 SILVIS WUI classes as well). Transects trace the path of a hypothetical incoming fire that ignites in the wildlands (left, Fig. 1, upper left Fig. 8A) and spreads into increasing densities of development and decreasing fuel densities (Right, Fig. 1, lower right Fig. 8A). The resulting exposure gradient has high points of building exposure as postulated at the outset of the study, although the peak is relative among the example gradients.

Relating our results to observed data is made difficult by the fact that most empirical studies of fire events focus on factors that consider loss, not exposure, and those that consider exposure may report results at varying levels of building density but not fuels, or vice versa. Results are presented in classes, where typically wildland vegetation is binned into large groups (Kramer et al., 2019; Mietkiewicz et al., 2020), confounding the ability to disentangle the gradient of burnable fuels and its effect on exposure. In other cases, both gradients of fuel and housing density (among other predictor variables) have been used to explain building exposure or loss (Penman et al., 2019; Price and Bradstock, 2013b), but are not presented in a way to allow for comparison to our results.

4.4. Study limitations and future improvements in wildfire disaster prediction

Despite the many limitations associated with simulation modeling and the methods in these experiments discussed above, the outputs from this work have useful application to prioritize federal, state, and local investments into community wildfire protection programs based on the level of exposure, source, and potential for forest management activities. We acknowledge limitations in the use of fire simulations for predicting building exposure and we have attempted to bridge our results with empirical data to mitigate over interpretation of the simulation data. Foremost, our predictions only apply to contemporary climate, which is not a well-founded assumption under a changing climate (Abatzoglou and Williams, 2016; Goss et al., 2020). Increasingly natural disaster assessments are incorporating climate change (Mills et al., 2018), although large scale spatial risk assessments for wildfire impacts under climate change in the US have not advanced to this stage (although see Syphard et al., 2019). Data vintages also make some of our comparisons coarse given simulation data represent 2014 fuels and the length of wind data records obtained from RAWS stations varied widely among pyromes with variable start dates as old as 1985. However, the sample size afforded by simulation, coupled with building footprint data with accuracy within a few meters makes it possible to characterize WUI exposure gradients at scales heretofore not possible for the conterminous US.

This study focused on wildfire disasters from a human context, and we recognize that uncharacteristic wildfires have cascading impacts on ecosystem processes and resiliency to other natural perturbations including climate. Well studied are the effects of extreme, stand-replacing wildfires that remove viable seed sources over large areas, create conditions that retard seedling establishment significantly delaying or preventing post-fire forest recovery (Kemp et al., 2016; Stephens et al., 2013), and converting forested areas into a qualitatively different vegetation type. Simulation modeling to map and predict these impacts and the potential benefits for restoration programs is well developed and complements the use of these models in the context of the present study. One major limitation of the simulation is that we do not measure exposure from firebrands transported beyond the fire perimeters (Koo et al., 2010) that expose buildings as potential ignition sources. Modeled wildfires do not burn into high-density WUI, whereas in actual fire events wildfires can spread through ember showers that ignite buildings and initiate building-to-building spread (e.g., 2014 Carlton Complex fire, WA; 2018 Carr Fire, CA) as discussed above. Building ignition from embers are a significant cause of loss, although in the current study where the concern is exposure the bias is due to embers being carried outside the final perimeter since we only measure final exposure within the fire perimeter (Koo et al., 2010).

Another potential interpretation problem stems from the scale differences between mapped fuels and FSim input fuelbeds. We expected significant under-prediction since simulated fires do not propagate into high-density developed areas where fuel beds are generally mapped as non-burnable. However, the resolution difference between the 30 m LANDFIRE data and the aggregated 270 m FSim fuels data biased predictions in both directions in areas that have highly intermixed fuel types. For instance, there are 81 30-m LANDFIRE pixels in one 270-m FSim pixel used in the simulations. If more than 40 pixels are classified as burnable fuels, FSim will burn in that pixel, and when overlaid with the MS building data, buildings will be exposed to fire using our methods, thus essentially allowing building exposure in areas with significant non-burnable surface fuels (e.g., 49%).

The relationship between historical rates of building loss relative to exposure varies widely among fire events and ecoregions (Alexandre et al., 2016a), making extrapolation of our exposure data to loss difficult at best. Kramer et al. (2019) reported a relatively stable loss rate among the WUI classes, ranging from 10 to 15%. Graham (2003) reported 17% building loss to wildfire for the 2002 Hayman fire, while Schmidt (2020) reported 41% for the 2015 Butte fire. Nonetheless, recent studies reported increasing loss rates in fires occurring after 2015 (Syphard and Keeley, 2019). At the extreme, the Camp fire destroyed a reported 96.2% (18,793 buildings; (Brown, 2020)) while many other fires have 0% reported loss (SIT 209). On average, across all the fires sampled in Alexandre et al. (2016a) from 2000 to 2010, percent building loss in the western US ecoregions was estimated at 20%. Detailed studies of building loss have identified local factors not considered in the current study including clustering, isolation, proximity to fuels, road density, and wind corridors (Syphard et al., 2017). In relation to building density, empirical studies report that loss was more likely if density was less than 54 km^{-2} (Syphard et al., 2017) or in the range of 0–12 structures km^{-2} (Syphard et al., 2019). Building density in Paradise, CA burned by the Camp fire was 361 km^{-2} (Syphard et al., 2019).

5. Conclusions

Both simulation and empirical studies can advance wildfire disaster prediction, and studies that synthesize information from both approaches will contribute to understanding and reducing wildfire losses to developed areas. In the future, simulation models that span the scale of landscapes to individual buildings will become widely available to predict large fire spread, propagation by non-wildland fuels into communities, and building ignition. New machine learning and remotely sensed data are available that can be used to construct individual building vulnerability models as done for predicting hurricane damage as a function of roof type (Bardeloza et al., 2019). Private sector insurance companies have developed prototype models that link landscape fire spread to ember production and building ignition models (Michael Young, Risk Management Solutions, pers. comm.) and applied these models to estimating expected financial loss from wildfires. Likewise, downscaled climate scenarios can be incorporated into mechanistic fire simulation models (Abatzoglou, 2013; Hulse et al., 2016) to assess future extreme wildfire events and their juxtaposition relative to developed areas. Work is underway to incorporate climate change into FSim using downscaled ERC generated from Global Circulation Models. These simulations will open the door to explore a wide range of management scenarios under alternative climate to understand how forest and fuel management investments, coupled with community hardening, can alter the current course of wildfire impacts. These and other enhancements will further advance the use of fire simulation modeling to predict future wildfire disasters and guide preventative programs in both the wildlands and within areas susceptible to them.

CRediT authorship contribution statement

Alan A. Ager: Conceptualization, Methodology, Writing – original draft, Writing – review & editing, Supervision, Funding acquisition. **Michelle A. Day:** Data curation, Investigation, Software, Writing –

original draft, Writing – review & editing, Visualization. **Fermin J. Alcasena:** Methodology, Formal analysis, Writing – review & editing. **Cody R. Evers:** Methodology, Visualization, Writing – review & editing. **Karen C. Short:** Methodology, Writing – review & editing. **Isaac Grenfell:** Methodology.

Declaration of competing interest

The authors declare that they have no known competing financial interests or personal relationships that could have appeared to influence the work reported in this paper.

Acknowledgements

Funding was provided by the USDA Forest Service National Fire Decision Support Center. We thank Ken Bunzel and Chris Ringo for help with GIS processing, Haiganoush Preisler for assistance with statistical modeling and two anonymous reviewers for their helpful comments.

Appendix A. Supplementary data

Supplementary data to this article can be found online at https://doi.org/10.1016/j.scitotenv.2021.147057.

References

Abatzoglou, J.T., 2013. Development of gridded surface meteorological data for ecological applications and modelling. Int. J. Climatol. 33, 121–131.
Abatzoglou, J.T., Williams, A.P., 2016. Impact of anthropogenic climate change on wildfire across western US forests. Proc. Natl. Acad. Sci. 113, 11770–11775.
Abatzoglou, J.T., Balch, J.K., Bradley, B.A., Kolden, C.A., 2018. Human-related ignitions concurrent with high winds promote large wildfires across the USA. Int. J. Wildland Fire 27, 377–386.
Abatzoglou, J.T., Williams, A.P., Barbero, R., 2019. Global emergence of anthropogenic climate change in fire weather indices. Geophys. Res. Lett. 46, 326–336.
Ager, A.A., Vaillant, N.M., Finney, M.A., 2011. Integrating fire behavior models and geospatial analysis for wildland fire risk assessment and fuel management planning. J. Comb. 19 572452.
Ager, A.A., Barros, A., Preisler, H.K., Day, M.A., Spies, T., Bailey, J., et al., 2017. Effects of accelerated wildfire on future fire regimes and implications for the United States federal fire policy. Ecol. Soc. 22, 12.
Ager, A.A., McMahan, A.J., Barrett, J.J., McHugh, C.W., 2007. A simulation study of thinning and fuel treatments on a wildland-urban interface in eastern Oregon, USA. Landsc. Urban Plan. 80, 292–300.
Ager, A.A., Palaiologou, P., Evers, C., Day, M.A., Ringo, C., Short, K.C., 2019. Wildfire exposure to the wildland urban interface in the western US. Appl. Geogr. 111, 102059.
Alcasena, F.J., Salis, M., Ager, A.A., Castell, R., Vega-Garcia, C., 2017. Assessing wildland fire risk transmission to communities in northern Spain. Forests 8, 27.
Alcasena, F.J., Ager, A.A., Bailey, J.D., Pineda, N., Vega-Garcia, C., 2019. Towards a comprehensive wildfire management strategy for Mediterranean areas: framework development and implementation in Catalonia, Spain. J. Environ. Manag. 231, 303–320.
Alexandre, P.M., Stewart, S.I., Keuler, N.S., Clayton, M.K., Mockrin, M.H., Bar-Massada, A., et al., 2016a. Factors related to building loss due to wildfires in the conterminous United States. Ecol. Appl. 26, 2323–2338.
Alexandre, P.M., Stewart, S.I., Mockrin, M.H., Keuler, N.S., Syphard, A.D., Bar-Massada, A., et al., 2016b. The relative impacts of vegetation, topography and spatial arrangement on building loss to wildfires in case studies of California and Colorado. Landsc. Ecol. 31, 415–430.
Angeler, D.G., Allen, C.R., Garmestani, A., Pope, K.L., Twidwell, D., Bundschuh, M., 2018. Resilience in environmental risk and impact assessment: concepts and measurement. Bull. Environ. Contam. Toxicol. 101, 543–548.
Attiwill, P.M., Adams, M.A., 2013. Mega-fires, inquiries and politics in the eucalypt forests of Victoria, south-eastern Australia. For. Ecol. Manag. 294, 45–53.
Badia, A., Pallares-Barbera, M., Valldeperas, N., Gisbert, M., 2019. Wildfires in the wildland-urban interface in Catalonia: vulnerability analysis based on land use and land cover change. Sci. Total Environ. 673, 184–196.
Bar Massada, A., Radeloff, V.C., Stewart, S.I., Hawbaker, T.J., 2009. Wildfire risk in the wildland–urban interface: a simulation study in northwestern Wisconsin. For. Ecol. Manag. 258, 1990–1999.
Barclay, E., 2019. This is a worst-possible wildfire scenario for Southern California. https://www.vox.com/2019/9/10/20804560/climate-change-california-wildfire-2019.
Bardeloza, D., Libatique, N.J., Tangonan, G.L., Vicente, M., Honrado, J., 2019. Towards vulnerability mapping on high resolution aerial images: roof detection, GIS, and machine learning techniques. 2019 IEEE Global Humanitarian Technology Conference (GHTC). IEEE, pp. 1–8.
Barrett, S., Havlina, D., Jones, J., Hann, W., Frame, C., Hamilton, D., et al., 2010. Interagency Fire Regime Condition Class Guidebook. Version 3.0. USDA Forest Service, US Department of Interior, and The Nature Conservancy Homepage of the Interagency Fire Regime Condition Class website.
Bhandary, U., Muller, B., 2009. Land use planning and wildfire risk mitigation: an analysis of wildfire-burned subdivisions using high-resolution remote sensing imagery and GIS data. J. Environ. Plan. Manag. 52, 939–955.
Bradshaw, L.S., Deeming, J.E., Burgan, R.E., Cohen, J.D., 1983. The 1978 National Fire-Danger Rating System: Technical Documentation. USDA Forest Service, Intermountain Forest and Range Experiment Station, Ogden, UT, p. 44.
Braziunas, K.H., Seidl, R., Rammer, W., Turner, M.G., 2020a. Can we manage a future with more fire? Effectiveness of defensible space treatment depends on housing amount and configuration. Landsc. Ecol. 36, 309–330.
Braziunas, K.H., Seidl, R., Rammer, W., Turner, M.G., 2020b. Can we manage a future with more fire? Effectiveness of defensible space treatment depends on housing amount and configuration. Landsc. Ecol. 1–22.
Brittain, S., 2015. Fire behavior FlamMap application interface. http://sbrittain.net/FB/FB_API.htm.
Brown, H., 2020. The camp fire tragedy of 2018 in California. Fire Management Today 78, 11–20.
CalFire, 2020. Camp Fire Structure Status. ESRI.
Calkin, D.E., Ager, A.A., Gilbertson-Day, J., Scott, J.H., Finney, M.A., Schrader-Patton, C., et al., 2010. Wildfire risk and hazard: procedures for the first approximation. USDA Forest Service, Rocky Mountain Research, Station, Fort Collins, CO, p. 62.
Calkin, D.E., Cohen, J.D., Finney, M.A., Thompson, M.P., 2014. How risk management can prevent future wildfire disasters in the wildland-urban interface. Proc. Natl. Acad. Sci. 111, 746–751.
Cansler, C.A., McKenzie, D., 2014. Climate, fire size, and biophysical setting control fire severity and spatial pattern in the northern Cascade Range, USA. Ecol. Appl. 24, 1037–1056.
Castellnou, M., Guiomar, N., Rego, F., Fernandes, P.M., 2018. Fire growth patterns in the 2017 mega fire episode of October 15, central Portugal. In: Viegas, D.X. (Ed.), Advances in Forest Fire Research, pp. 447–453.
Charnley, S., Kelly, E.C., Fischer, A.P., 2020. Fostering collective action to reduce wildfire risk across property boundaries in the American West. Environ. Res. Lett. 15, 025007.
Chas-Amil, M.-L., García-Martínez, E., Touza, J., 2020. Iberian Peninsula October 2017 wildfires: burned area and population exposure in Galicia (NW of Spain). Int. J. Disaster Risk Reduction 48, 101623.
Chen, K., McAneney, J., 2004. Quantifying bushfire penetration into urban areas in Australia. Geophys. Res. Lett. 31.
Clark, A.M., Rashford, B.S., McLeod, D.M., Lieske, S.N., Coupal, R.H., Albeke, S.E., 2016. The impact of residential development pattern on wildland fire suppression expenditures. Land Econ. 92, 656–678.
Coop, J.D., Parks, S.A., Stevens-Rumann, C.S., Crausbay, S.D., Higuera, P.E., Hurteau, M.D., et al., 2020. Wildfire-driven forest conversion in western North American landscapes. BioScience 70, 659–673.
Cruz, M.G., Alexander, M.E., 2013. Uncertainty associated with model predictions of surface and crown fire rates of spread. Environ. Model Softw. 47, 16–28.
Cruz, M.G., Sullivan, A.L., Gould, J.S., Sims, N.C., Bannister, A.J., Hollis, J.J., et al., 2012. Anatomy of a catastrophic wildfire: the Black Saturday Kilmore East fire in Victoria, Australia. For. Ecol. Manag. 284, 269–285.
Dillon, G.K., 2015. Wildfire Hazard Potential (WHP) for the Conterminous United States (270-M GRID), Version 2014 Continuous. Forest Service Research Data Archive, Fort Collins, CO.
Donato, D.C., Halofsky, J.S., Reilly, M.J., 2020. Corralling a black swan: natural range of variation in a forest landscape driven by rare, extreme events. Ecol. Appl. 30, e02013.
Dye, A.W., Kim, J.B., McEvoy, A., Fang, F., Riley, K.L., 2021. Evaluating rural Pacific Northwest towns for wildfire evacuation vulnerability. Nat. Hazards https://doi.org/10.1007/s11069-021-04615-x.
ESRI, 2012. North America Detailed Streets.
Evers, C., Ager, A.A., Nielsen-Pincus, M., Palaiologou, P., Bunzel, K., 2019. Archetypes of community wildfire exposure from national forests in the western US. Landsc. Urban Plan. 182, 55–66.
Feller, W., 1968. An Introduction to Probability Theory and its Applications. John Wiley and Sons, New York.
Finney, M.A., 2002. Fire growth using minimum travel time methods. Can. J. For. Res. 32, 1420–1424.
Finney, M.A., Grenfell, I.C., McHugh, C.W., 2009. Modeling containment of large wildfires using generalized linear mixed model analysis. For. Sci. 55, 249–255.
Finney, M.A., McHugh, C.W., Grenfell, I.C., Riley, K.L., Short, K.C., 2011. A simulation of probabilistic wildfire risk components for the continental United States. Stoch. Env. Res. Risk A. 25, 973–1000.
Fischer, A.P., Kline, J.D., Ager, A.A., Charnley, S., Olsen, K.A., 2014. Objective and perceived wildfire risk and its influence on private forest landowners' fuel reduction activities in Oregon's (USA) ponderosa pine ecoregion. Int. J. Wildland Fire 23, 143–153.
Fischer, A.P., Spies, T.A., Steelman, T.A., Moseley, C., Johnson, B.R., Bailey, J.D., et al., 2016. Wildfire risk as a socioecological pathology. Front. Ecol. Environ. 14, 277–285.
Gabbert, B., 2020. Where Did the Term "Gigafire" Originate? Wildfire Today
Ghasemi, B., Kyle, G.T., Absher, J.D., 2020. An examination of the social-psychological drivers of homeowner wildfire mitigation. J. Environ. Psychol. 70, 101442.
Gibbons, P., Van Bommel, L., Gill, A.M., Cary, G.J., Driscoll, D.A., Bradstock, R.A., et al., 2012. Land management practices associated with house loss in wildfires. PLoS One 7, e29212.
Goss, M., Swain, D.L., Abatzoglou, J.T., Sarhadi, A., Kolden, C.A., Williams, A.P., et al., 2020. Climate change is increasing the likelihood of extreme autumn wildfire conditions across California. Environ. Res. Lett. 15, 094016.
Graham, R.T., 2003. Hayman Fire Case Study. USDA Forest Service, Rocky Mountain Research Station, Ogden, UT, p. 396.

Grenfell, I.C., Finney, M., Jolly, M., 2010. Simulating spatial and temporally related fire weather. In: Viegas, D. (Ed.), Proceedings of the VI International Conference on Forest Fire Research. University of Coimbra, Coimbra, Portugal.

Gude, P.H., Jones, K., Rasker, R., Greenwood, M.C., 2013. Evidence for the effect of homes on wildfire suppression costs. Int. J. Wildland Fire 22, 537–548.

Haas, J.R., Calkin, D.E., Thompson, M.P., 2013. A national approach for integrating wildfire simulation modeling into WIldland Urban Interface risk assessments within the United States. Landsc. Urban Plan. 119, 44–53.

Hulse, D., Branscomb, A., Enright, C., Johnson, B., Evers, C., Bolte, J., et al., 2016. Anticipating surprise: using agent-based alternative futures simulation modeling to identify and map surprising fires in the Willamette Valley, Oregon USA. Landsc. Urban Plan. 156, 26–43.

Irikura, K., Miyake, H., 2011. Recipe for predicting strong ground motion from crustal earthquake scenarios. Pure Appl. Geophys. 168, 85–104.

Joseph, M.B., Rossi, M.W., Mietkiewicz, N.P., Mahood, A.L., Cattau, M.E., St. Denis, L.A., et al., 2019. Spatiotemporal prediction of wildfire size extremes with Bayesian finite sample maxima. Ecol. Appl. 29, e01898.

Keeley, J.E., Syphard, A.D., 2019. Twenty-first century California, USA, wildfires: fuel-dominated vs. wind-dominated fires. Fire Ecol. 15.

Keeley, J.E., Rubin, G., Brennan, T., Piffard, B., 2020. Protecting the wildland-urban interface in California: greenbelts vs thinning for wildfire threats to homes. Bull. South. Calif. Acad. Sci. 119, 35–47.

Kemp, K.B., Higuera, P.E., Morgan, P., 2016. Fire legacies impact conifer regeneration across environmental gradients in the US northern Rockies. Landsc. Ecol. 31, 619–636.

Kerns, B.K., Tortorelli, C., Day, M.A., Nietupski, T., Barros, A.M.G., Kim, J.B., et al., 2020. Invasive grasses: a new perfect storm for forested ecosystems? For. Ecol. Manag. 463, 117985.

Koo, E., P.J, P., Weise, D.R., Woycheese, J.P., 2010. Firebrands and spotting ignition in large-fires. Int. J. Wildland Fire 19, 818–843.

Kramer, H.A., Mockrin, M.H., Alexandre, P.M., Stewart, S.I., Radeloff, V.C., 2018. Where wildfires destroy buildings in the US relative to the wildland–urban interface and national fire outreach programs. Int. J. Wildland Fire 27, 329–341.

Kramer, H.A., Mockrin, M.H., Alexandre, P.M., Radeloff, V.C., 2019. High wildfire damage in interface communities in California. Int. J. Wildland Fire 28, 641.

Kulig, J., Botey, A.P., 2016. Facing a wildfire: what did we learn about individual and community resilience? Nat. Hazards 82, 1919–1929.

Lambert, J.H., Li, D., Haimes, Y.Y., 1994. Risk of extreme flood losses under uncertain physical conditions. Engineering Risk in Natural Resources Management. Springer, pp. 321–329.

LANDFIRE, 2014. Homepage of the LANDFIRE Project. http://www.landfire.gov/index.php.

LANDFIRE, 2017. 40 Scott and Burgan Fire Behavior Fuel Models. LF 1.4.0. Refresh. US Department of Interior, Geological Survey.

Littell, J.S., Peterson, D.L., Riley, K.L., Liu, Y.Q., Luce, C.H., 2016. A review of the relationships between drought and forest fire in the United States. Glob. Chang. Biol. 22, 2353–2369.

Liu, Y., Stanturf, J., Goodrick, S., 2010. Trends in global wildfire potential in a changing climate. For. Ecol. Manag. 259, 685–697.

Makridakis, S., Taleb, N., 2009. Living in a world of low levels of predictability. Int. J. Forecast. 25, 840–844.

Maranghides, A., Mell, W., 2011. A case study of a community affected by the Witch and Guejito wildland fires. Fire. Technol 47, 379–420.

Martin, W.E., Martin, I.M., Kent, B., 2009. The role of risk perceptions in the risk mitigation process: the case of wildfire in high risk communities. J. Environ. Manag. 91, 489–498.

Martinuzzi, S., Stewart, S.I., Helmers, D.P., Mockrin, M.H., Hammer, R.B., Radeloff, V.C., 2015. In: Service, U.F. (Ed.), The 2010 Wildland-Urban Interface of the Conterminous United States - Geospatial Data Fort Collins, CO.

Microsoft, 2018. Computer Generated Building Footprints for the United States GitHub Repository.

Mietkiewicz, N., Balch, J.K., Schoennagel, T., Leyk, S., St Denis, L.A., Bradley, B.A., 2020. In the line of fire: consequences of human-ignited wildfires to homes in the US (1992–2015). Fire. 3, 50.

Miller, C., Ager, A.A., 2013. A review of recent advances in risk analysis for wildfire management. Int. J. Wildland Fire 22, 1–14.

Mills, D., Jones, R., Wobus, C., Ekstrom, J., Jantarasami, L., St Juliana, A., et al., 2018. Projecting age-stratified risk of exposure to inland flooding and wildfire smoke in the United States under two climate scenarios. Environ. Health Perspect. 126, 047007.

Morgan, P., Hardy, C.C., Swetnam, T.W., Rollins, M.G., Long, D.G., 2001. Mapping fire regimes across time and space: understanding coarse and fine-scale fire patterns. Int. J. Wildland Fire 10, 329–342.

MTBS Data Access, 2020a. MTBS Data Access: burned areas boundaries, 1984–2018. MTBS Project (USDA Forest Service/US Geological Survey).

MTBS Data Access, 2020b. MTBS Data Access: fire occurrence dataset, 1984–2018. MTBS Project (USDA Forest Service/US Geological Survey).

Nagy, R., Fusco, E., Bradley, B., Abatzoglou, J.T., Balch, J., 2018. Human-related ignitions increase the number of large wildfires across US ecoregions. Fire. 1, 4.

Noonan-Wright, E.K., Opperman, T.S., Finney, M.A., Zimmerman, G.T., Seli, R.C., Elenz, L.M., et al., 2011. Developing the US wildland fire decision support system. J. Comb. 14 168473.

Norris, F.H., Stevens, S.P., Pfefferbaum, B., Wyche, K.F., Pfefferbaum, R.L., 2008. Community resilience as a metaphor, theory, set of capacities, and strategy for disaster readiness. Am. J. Community Psychol. 41, 127–150.

O'Connor, C.D., Falk, D.A., Lynch, A.M., Swetnam, T.W., 2014. Fire severity, size, and climate associations diverge from historical precedent along an ecological gradient in the Pinaleño Mountains, Arizona, USA. For. Ecol. Manag. 329, 264–278.

Oliveira, S., Gonçalves, A., Benali, A., Sá, A., Zêzere, J.L., Pereira, J.M., 2020. Assessing risk and prioritizing safety interventions in human settlements affected by large wildfires. Forests. 11, 859.

Omernik, J.M., 1987. Ecoregions of the Coterminous United States. Map (scale 1: 7,500,000). Ann. Assoc. Am. Geogr. 77, 118–125.

Parisien, M.A., Barber, Q.E., Hirsch, K.G., Stockdale, C.A., Erni, S., Wang, X., et al., 2020. Fire deficit increases wildfire risk for many communities in the Canadian boreal forest. Nat. Commun. 11, 2121.

Parks, S.A., Miller, C., Holsinger, L.M., Baggett, L.S., Bird, B.J., 2016. Wildland fire limits subsequent fire occurrence. Int. J. Wildland Fire 25, 182–190.

Penman, T.D., Collins, L., Syphard, A.D., Keeley, J.E., Bradstock, R.A., 2014. Influence of fuels, weather and the built environment on the exposure of property to wildfire. PLoS One 9, e111414.

Penman, T.D., Nicholson, A.E., Bradstock, R.A., Collins, L., S.H, P., Price, O.F., 2015. Reducing the risk of house loss due to wildfires. Environ. Model Softw. 67, 12–25.

Penman, S.H., Price, O.F., Penman, T.D., Bradstock, R.A., 2019. The role of defensible space on the likelihood of house impact from wildfires in forested landscapes of south eastern Australia. Int. J. Wildland Fire 28, 4–14.

Peterson, D.A., Hyer, E.J., Campbell, J.R., Fromm, M.D., Hair, J.W., Butler, C.F., et al., 2015. The 2013 rim fire: implications for predicting extreme fire spread, pyroconvection, and smoke emissions. Bull. Am. Meteorol. Soc. 96, 229–247.

Price, O.F., Bradstock, R.A., 2013a. Landscape scale influences of forest area and housing density on house loss in the 2009 Victorian bushfires. PLoS One 8, e73421.

Price, O.F., Bradstock, R.A., 2013b. The spatial domain of wildfire risk and response in the wildland urban interface in Sydney, Australia. Nat. Hazards Earth Syst. Sci. 13, 3385–3393.

Price, O., Borah, R., Bradstock, R., Penman, T., 2015. An empirical wildfire risk analysis: the probability of a fire spreading to the urban interface in Sydney, Australia. Int. J. Wildland Fire 24, 597–606.

Prichard, S.J., Stevens-Rumann, C.S., Hessburg, P.F., 2017. Tamm review: shifting global fire regimes: lessons from reburns and research needs. For. Ecol. Manag. 396, 217–233.

R Core Team, 2019. R: A Language and Environment for Statistical Computing. R Foundation for Statistical Computing, Vienna, Austria.

Radeloff, V.C., Hammer, R.B., Stewart, S.I., Fried, J.S., Holcomb, S.S., McKeefry, J.F., 2005. The wildland-urban interface in the United States. Ecol. Appl. 15, 799–805.

Radeloff, V.C., Helmers, D.P., Kramer, H.A., Mockrin, M.H., Alexandre, P.M., Bar-Massada, A., et al., 2018. Rapid growth of the US wildland-urban interface raises wildfire risk. Proc. Natl. Acad. Sci. 115, 3314–3319.

Riley, K.L., Thompson, M.P., Scott, J.H., Gilbertson-Day, J.W., 2018. A model-based framework to evaluate alternative wildfire suppression strategies. Resources. 7, 4.

Sajjad, M., Chan, J.C., 2019. Risk assessment for the sustainability of coastal communities: a preliminary study. Sci. Total Environ. 671, 339–350.

Sajjad, M., Lin, N., Chan, J.C.L., 2020. Spatial heterogeneities of current and future hurricane flood risk along the U.S. Atlantic and Gulf coasts. Sci. Total Environ. 713, 136704.

Schmidt, J., 2020. The Butte Fire: A Case Study in Using LIDAR Measures of Pre-Fire Vegetation to Estimate Structure Loss Rates. Munich Personal RePEc Archive.

Schoennagel, T., Balch, J.K., Brenkert-Smith, H., Dennison, P.E., Harvey, B.J., Krawchuk, M.A., et al., 2017. Adapt to more wildfire in western North American forests as climate changes. Proc. Natl. Acad. Sci. U. S. A. 114, 4582–4590.

Scott, J., Helmbrecht, D., Thompson, M.P., Calkin, D.E., Marcille, K., 2012. Probabilistic assessment of wildfire hazard and municipal watershed exposure. Nat. Hazards 64, 707–728.

Scott, J.H., Thompson, M.P., Calkin, D.E., 2013. A Wildfire Risk Assessment Framework for Land and Resource Management. USDA Forest Service, Rocky Mountain Research Station, Fort Collins, CO, p. 83.

Short, K.C., Finney, M.A., Vogler, K., Scott, J.H., Gilbertson-Day, J.W., Julie, W., et al., 2020a. Spatial Datasets of Probabilistic Wildfire Risk Components for the United States (270 m). 2nd edition. Forest Service Research Data Archive, Fort Collins, CO.

Short, K.C., Grenfell, I.C., Riley, K.L., Vogler, K., 2020b. Pyromes of the Conterminous United States. Forest Service Research Data Archive, Fort Collins, CO.

SILVIS Lab, 2012. 2010 Wildland Urban Interface (WUI) Maps. University of Wisconsin, Madison, WI.

St Denis, L.A., Mietkiewicz, N.P., Short, K.C., Buckland, M., Balch, J.K., 2020. All-hazards dataset mined from the US National Incident Management System 1999–2014. Sci. Data. 7, 64.

Stavros, E.N., Abatzoglou, J.T., McKenzie, D., Larkin, N.K., 2014. Regional projections of the likelihood of very large wildland fires under a changing climate in the contiguous Western United States. Clim. Chang. 126, 455–468.

Steelman, T., 2016. U.S. wildfire governance as a social-ecological problem. Ecol. Soc. 21, 3.

Stephens, S.L., Agee, J.K., Fule, P.Z., North, M.P., Romme, W.H., Swetnam, T.W., et al., 2013. Managing forests and fire in changing climates. Science 342, 41–42.

Syphard, A., Keeley, J.E., 2019. Factors associated with structure loss in the 2013–2018 California wildfires. Fire. 2.

Syphard, A.D., Keeley, J.E., Massada, A.B., Brennan, T.J., Radeloff, V.C., 2012. Housing arrangement and location determine the likelihood of housing loss due to wildfire. PLoS One 7, e33954.

Syphard, A.D., Brennan, T.J., Keeley, J.E., 2014. The role of defensible space for residential structure protection during wildfires. Int. J. Wildland Fire 23, 1165–1175.

Syphard, A.D., Brennan, T.J., Keeley, J.E., 2017. The importance of building construction materials relative to other factors affecting structure survival during wildfire. Int. J. Disaster Risk Reduction 21, 140–147.

Syphard, A.D., Rustigian-Romsos, H., Mann, M., Conlisk, E., Moritz, M.A., Ackerly, D., 2019. The relative influence of climate and housing development on current and projected future fire patterns and structure loss across three California landscapes. Glob. Environ. Chang. 56, 41–55.

Taleb, N.N., 2007. The Black Swan: The Impact of the Highly Improbable. vol. 2. Random house, New York.
Tedim, F., Leone, V., Amraoui, M., Bouillon, C., Coughlan, M.R., Delogu, G.M., et al., 2018. Defining extreme wildfire events: difficulties, challenges, and impacts. Fire. 1, 9.
Thompson, M., Scott, J., Langowski, P., Gilbertson-Day, J., Haas, J., Bowne, E., 2013. Assessing watershed-wildfire risks on National Forest System lands in the Rocky Mountain Region of the United States. Water 5, 945–971.
Thurston, W., Kepert, J.D., Tory, K.J., Fawcett, R.J., 2017. The contribution of turbulent plume dynamics to long-range spotting. Int. J. Wildland Fire 26, 317–330.
Toman, E., Shindler, B., McCaffrey, S., Bennett, J., 2014. Public acceptance of wildland fire and fuel management: panel responses in seven locations. Environ. Manag. 54, 557–570.
Turco, M., Jerez, S., Augusto, S., Tarín-Carrasco, P., Ratola, N., Jiménez-Guerrero, P., et al., 2019. Climate drivers of the 2017 devastating fires in Portugal. Sci. Rep. 9, 1–8.
United Nations, 2015. Sendai Framework for Disaster Risk Reduction 2015–2030. p. 32.
US Census Bureau, 2016. USA Census populated places areas. Esri Data & Maps. ESRI.
US Environmental Protection Agency, 2019. Level I Ecoregions of North America. US EPA.
USGS, 2011. National Land Cover Database 2011 Land Cover (CONUS). US Geological Survey, Earth Resources Observation and Science (EROS) Center.
USGS, 2016. Protected Areas Database of the United States (PAD-US). USGS Gap Analysis Program (GAP).
Vickery, P., Skerlj, P., Twisdale, L., 2000. Simulation of hurricane risk in the US using empirical track model. J. Struct. Eng. 126, 1222–1237.
Viegas, D., 2013. Are Extreme Forest Fires the New Normal? The Conversation